A Biologically Accurate 3D Model of the Locomotion of *Caenorhabditis Elegans*

Roger Mailler, Jason Avery, Jacob Graves, and Nathan Willy
Computational Neuroscience and Adaptive Systems Laboratory
University of Tulsa
Tulsa, United States
{*mailler, jason-avery, jacob-graves, nathan-willy*}*@utulsa.edu*

***Abstract*—The nematode *Caenorhabditis Elegans* has become an important model organism for many areas of biological research including genetics, development, and neurobiology. It is the first organism to have its genome sequenced, complete cell ontogeny determined, and nervous system mapped. With all of the information that is available on this simple organism, *C. elegans* may also become the first organism to be accurately and completely modeled *in silico*.**

In this work we take a step toward this goal by presenting a biologically accurate, 3-dimensional model of *C. elegans*. This model takes into account many facets of the organism including size, shape, weight distribution, muscle placement, and muscle force. We also explicitly model the environment of the worm to include factors such as contact, friction, inertia, and gravity.

We tuned and validated our model using video recordings taken of the worm and show that our model accurately depicts the physics of undulatory locomotion used to forward crawl on an agarose surface. We also present evidence that suggests that the forces applied by the nematode during locomotion are not uniform, but decrease as the wave is propagated from its head to its tail.

***Keywords*-Simulation, Biology, *Caenorhabditis elegans*, Modeling**

I. Introduction

Nearly 50 years ago, Sydney Brenner introduced *Caenorhabditis Elegans* as a model for studying developmental biology and neurology. Because of its simplicity, it has become one of the best understood organisms on the planet being the only one to have its cell lineage, genome, and nervous system completely mapped. However, despite all of the effort that has gone into uncovering the secrets behind "the mind of the worm," we still lack a compelling systems-level understanding for how the neurons and the connections between them generate the surprisingly complex range of behaviors that are observed in this relatively simple organism.

One potential approach to addressing this issue is to use computer simulations that model aspects of the worm's body and nervous system. For example, numerous computer simulations have been created that replicate the locomotion of *C. elegans* [11], [9], [17], [4].

Like all models, these simulations make simplifying assumptions that make them computationally tractable at the expense of accuracy. Each of them, for instance, represents the body as a set of uniformly distributed points in two-dimensional space. This prevents them from replicating the proper weight distribution, and more importantly, the non-uniform placement of the muscles that are used to generate locomotive force in the actual worm. In addition, they also fail to directly simulate the environment, but instead apply constant frictional forces at these discrete points along the body. This simplifying assumption limits the ability of these simulations to accurately depicting the non-uniform friction that results from the worm's contact with the world around it. This work seeks to rectify these deficiencies by developing a biologically accurate 3D model of the body of *C. elegans* in a virtual environment that mirrors the physical properties of its natural world. This simulator, which has been under development for over a year, is built using an open-source 3D game and physics engine. The model accurately depicts the physical properties of the real organism including its non-uniform weight, size, shape, and musculature. In addition, the simulator models the interaction between the worm and its environment to include contact, friction, inertia, and gravity.

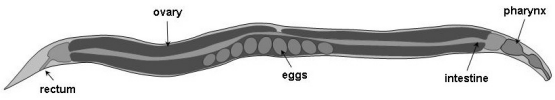

Figure 1. Basic anatomy of an adult hermaphrodite.

This paper presents this new model and demonstrates that it faithfully reproduces forward crawling of *C. elegans* on an agarose surface. The model is cross validated using video recording of worms during forward crawling that were converted to quantitative data by image analysis software. During our validation, we found that forces generated by the muscles may decrease as the wave propagates from the worm's head to its tail. Although we found no mention of this in the literature, the placement of the muscles in the worm's body, along with video analysis of the worm's crawling gait seem to support our finding.

II. *Caenorhabditis Elegans*

Caenorhabditis elegans is a small (1 millimeter in length) nematode that can be found living in the soil of many parts

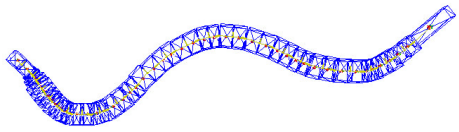

Figure 2. Physics model of the nematode *C. elegans*

of the world. It lives by feeding on bacteria and is capable of reproducing in about 3 days under the right conditions. *C. elegans* can either be male or hermaphrodite, with males occurring at a low frequency in the population. They reproduce by either self fertilization in the hermaphrodite or by mating a male and hermaphrodite. Hermaphrodites lay about 300 eggs during their approximately 15 day lifespan.

C. elegans (see Figure **??**) is a very simple organism, with only 959 cells in the adult hermaphrodite and 1031 in the adult male [18]. Like other members of the nematode (Nematoda) family, the body of *C. elegans* is composed of two concentric tubes separated by a pseudocoelom. The inner tube is in the intestine and the outer tube consists of the hypodermis, muscles, nerves and the gonads. The pseudocoelom is filled with a hydrostatically pressurized fluid that helps maintain the shape of its body.

C. elegans maintains an outer cuticle, which is secreted by the hypodermis. During the lifespan of the worm, it molts its cuticle four times, punctuating the four phases of its life cycle. The cuticle, containing mostly collagen, is tough although not rigid. Adult nematodes have lateral, longitudinal seam cells on the surface of their cuticle that form treads (alae). When on a solid surface, the nematode crawls on one side with a set of treads contacting the surface.

A. Locomotion

The main body wall muscles of *C. elegans* are arranged in four rows, two dorsal and two ventral. Each row consists of 23 or 24 muscle cells that are arranged in an interleaving pattern [6]. Toward the anterior of the worm, the cells occur in overlapping pairs with less overlap and pairing occurring toward the posterior. The worm moves by propagating waves either forward or backward along its body creating a sinusoidal pattern of locomotion.

III. Simulator

To develop the core simulation framework, we chose to use a Java-based high performance 3D game engine called the Java Monkey Engine (JME) [13]. Originally created by Mark Powell, JME provides all of the major features found in commercial quality game engines including loading and manipulation of 3D meshes, lighting and shadows, sound effects, animation, and terrain. JME uses a scene graph based API that allows developers to easily modify composed objects in their scene and the game engine to quickly cull branches of the graph during rendering. This makes it both easy to use and exceptionally fast.

Table I
Body segment sizes (all numbers in μm)

i	l_i	r_i	**i**	l_i	r_i	**i**	l_i	r_i
1	50	24	**10**	45	40	**19**	35	40
2	10	28	**11**	30	40	**20**	50	40
3	15	34	**12**	55	40	**21**	55	40
4	25	40	**13**	40	40	**22**	30	40
5	20	40	**14**	50	40	**23**	40	38
6	25	40	**15**	40	40	**24**	50	32
7	20	40	**16**	50	40	**25**	100	24
8	40	40	**17**	55	40			
9	30	40	**18**	40	40			

At the core of our simulation framework is the Open Dynamics Engine (ODE) [15], which interfaces with JME using JME Physics [14]. ODE is designed to simulate articulated rigid body physics. Objects in the simulation are built from various 3D shapes that are connected to one another by joints. ODE allows users to specify the properties of the objects including weight, surface friction, and center of gravity. Joints can be created between the objects and up to six degrees of freedom are supported.

ODE uses a highly stable, first-order implicit Euler integrator. Although not quite as accurate as a fourth-order Runge-Kutta integrator, it is remarkably fast and with small enough time steps provides very realistic physical approximations. ODE handles contact and friction using a version of the Dantzig Linear Complementarity Problem (LCP) solver that was described in [**?**]. However, it uses a faster Coloumb friction model to optimize speed. ODE is used in a number of research and commercial robotics simulators including Gazebo [**?**], Marilou [**?**], and Webots [**?**].

A. Physics Model

Because ODE is designed to simulate rigid objects, we modeled the body as set of 25 discrete segments $S_i = \{1, \cdots, 25\}$ (see Figure 1). As a notational convenience we refer to segments by their index number and use the subscript i in equations to denote the segment S_i. Each segment is represented using a 3D box whose width and height are estimated by the radius, r_i, taken from photographs of living worms and length, l_i, are given by the spacing between subsequent muscle cell locations along the worm's anterior-posterior axis (see Table I). These muscle cell locations, which are taken from [16], represent the main points of powered articulation along the body .

The volume of each segment can be calculated by

$$v_i = 4r_i^2 \times l_i \tag{1}$$

and their mass, w_i, is a fraction of the total mass W and can be calculated by

$$w_i = \frac{W \times v_i}{v_{total}} \tag{2}$$

This representation creates non-uniform weights and sizes for the individual sections of the worm. This, in turn,

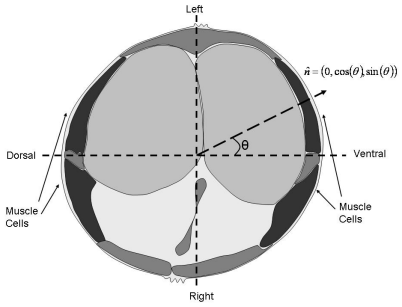

Figure 3. Cross-section showing the location of the muscle cells

Table II
PARAMETERS USED IN THE SIMULATION

Parameter	Description	Value	Units
L	Total length of the body	1000	μm
W	Total mass of the body	$5 \cdot 10^{-9}$	kg
F_m^{max}	Max muscle cell force	$2.5 \cdot 10^{-12}$	N
θ_m^{max}	Max muscle cell bend	$\frac{\pi}{10}$	rad
k_s	Torsional spring constant	$10 \cdot 10^{-12}$	$N \cdot m/rad$
k_p	Torsional pressure constant	$0.63 \cdot 10^{-12}$	$N \cdot m/rad$
b	Torsional damping constant	$0.2 \cdot 10^{-12}$	$N \cdot m \cdot s/rad$
μ_l	Coefficient of lateral friction	10	
μ_a	Coefficient of axial friction	1×10^{-1}	
λ	CPG wavelength	22	joints
Δt	CPG update interval	150	ms

impacts the shape and frictional properties associated with the contact surface between the worm and its environment.

Subsequent segments of the body, S_i and S_{i+1}, are connected to one another by a powered rotational joint, J_k. Like segments, we use the notational convenience of referring to the joint by its index number and use the subscript k to denote joint J_k. These joints have 2 degrees of freedom and have an angle at time t that is represented as a 3D vector $\vec{\theta}_k(t)$. The angular velocity of this joint $\vec{v}_k(t)$, is also represented as a vector with each element being the change in the corresponding angle over time.

The values of $\vec{\theta}_k(t)$ and $\vec{v}_k(t)$ are calculated by the underlying physics engine based on the various forces that are acting on the joint and the segments they connect. This is the topic of the next section.

B. Dynamics

At any given time there are a number of forces that act on the body of the worm. These include gravity, friction, inertia, elastic forces from the cuticle, force associated with internal pressure, dampening forces caused by the incompressibility of liquid, and forces exerted by the muscles.

Fortunately, ODE handles gravitational, inertial, and frictional forces that act on the worm by allowing users to specify the mass (for computing gravitational and inertial forces) and the size, shape, and frictional coefficients for each of the segments of the body (for computing frictional forces). Tables I and II list the values that are used in our simulation.

The forces that act on the joints are computed by our model about 100 times per second during each update of the physics model. The total force applied to a joint J_k at time t is calculated using the following equation:

$$\vec{F}_k^T(t) = \vec{F}_k^M(t) + \vec{F}_k^S(t) + \vec{F}_k^P(t) + \vec{F}_k^D(t) \qquad (3)$$

where $\vec{F}_k^M$ is the force exerted by the muscles, $\vec{F}_k^S$ is the force exerted by the elastic cuticle, $\vec{F}_k^P$ is the force exerted by the interior hydrostatic pressure, and $\vec{F}_k^D$ is a dampening force.

1) Muscle Forces: Muscle forces in *C. elegans* are produced by muscle cells that are attached to the cuticle of the body. These cells are arranged parallel to the anterior-posterior (AP) axis of the body in four rows with two rows on the dorsal and two rows on the ventral side. Figure 2 show a cross section of *C. elegans* showing the location of the muscles cells approximately half way down the AP axis. As can be seen in this figure, the muscle cells are offset by approximately 30 degrees left and right of the dorsal-ventral midline. Muscle cells are, therefore, named based on their AP position in the row and the row's position relative to the dorsal-ventral and left-right mid-lines. For example , the 7th muscle cell in the dorsal, right row is called MDR07. For simplicity, we refer to the set of muscle cells located at joint k as $m_k = \{MDL_k, MDR_k, MVL_k, MVR_k\}$.

For most of the worm's body, this offset has very little effect because the innervation pattern activates both the left and right muscle cells on a single side of the worm at the same time. This is not true in the head where a more complex innervation pattern allows the worm to lift its head by activating the muscle on the left or right side at the same time.

We accounted for the offset placement of the muscle cells by calculating the force generated by each cell independently and multiplying that force by $\hat{\mathbf{n}}$, which is a unit vector normal to the surface of the worm. The normal vector is easily computed by $\hat{\mathbf{n}} = (\mathbf{0}, \pm\cos(\theta), \pm\sin(\theta))$ with signs being set appropriately according to quadrant location of the muscle cell. The following equation is used to calculate the muscle force applied to joint k at time t:

$$\vec{F}_k^M(t) = \sum_{m \in m_k} a_m \times F_m(\vec{\theta}_k(t)) * \hat{\mathbf{n}} \qquad (4)$$

In the equation, a_m is the current activation level, a graded signal, of the muscle based on the inputs from the neurons innervating muscle cell m and $F_m(\vec{\theta}_k(t))$ is the maximum force that the cell can produce given its current length.

To compute $F_m(\vec{\theta}_k(t))$, we used a linear approximation to the Hill equation for the force/length relationship of muscle cells [8].

$$F_m(\vec{\theta}_k(t)) = (0.5k_s - \frac{F_m^{max}}{\theta_m^{max}}) \times |\vec{\theta}_k(t)| + F_m^{max} \qquad (5)$$

Here, F_m^{max} is the maximum force that the cell produces at

resting length, θ_m^{max} is the maximum angle that the joint can be displaced as a result of the contraction of the muscle and k_s is the spring constant associated with the elastic cuticle. The slope of this line is based on the spring constant of the cuticle such that these forces come to equilibrium when $|\vec{\theta}_k(t)| = \theta_m^{max}$ and both the right and left muscle are fully activated. This, by no means, limits the maximum bend angle of the joint. Both external and inertial forces can cause a joint to exceed θ_m^{max}. The values for these constants (Table II) were chosen based on values from [2] and [17] and were tuned using videos of worms during forward locomotion (see Section IV).

2) Spring, Pressure, and Damping forces: Whereas muscle force causes the body to deviate from it resting state, there are a number of forces that act to restore it. One of these forces is the elasticity of the cuticle, which can be modeled as a simple spring. Below is the equation for the force exerted by this spring:

$$\vec{F}_k^S(t) = -0.8 \times k_s \times \vec{\theta}_k(t) \tag{6}$$

The value for k_s is strongly related to the maximum muscle force and was chosen to be $k_s = 4 * F_m^{max}$. This creates a relationship between these values such that the average force applied over the range of dorsal or ventral muscle contraction is $\frac{1}{2}F_m^{max}$.

Along with the force created by the cuticle, internal pressure of the worm's body also exerts a restorative force. Recent measurements of the relationship between the elastic cuticle and the hydrostatic pressure using a piezoresistive displacement clamp have shown that the restorative force has a cuticle to pressure force ratio of 4 to 1 [12]. We used these finding to normalize the force associated with these two factors. Below is the equation we use for calculating the force associated with internal pressure:

$$\vec{F}_k^P(t) = -0.2 \times k_s \times \theta_m^{max} \tag{7}$$

We explicitly do not model the relationship between the change in volume and pressure as the body bends. We ignored this factor because it has been reported that total body volume does not change significantly over the worm's range of motion [11], [17]. This indicates that pressure acts a constant, not dynamic, restorative property, so we treat it as such.

Lastly, because of the structure and composition of the worm's body, it acts like a fluid-filled shock absorber. So, we apply a damping force to model the resistance that the body has to rapid changes in position using the formula below:

$$\vec{F}_k^D(t) = -b \times \vec{v}_k(t) \tag{8}$$

The value for b was derived through experimentation and is in line with value reported in [17].

Table III
SYNAPTIC WEIGHTS USED IN THE SIMULATION

k	ω_k	k	ω_k	k	ω_k	k	ω_k
1	0.45	**7**	1.00	**13**	1.00	**19**	0.50
2	0.55	**8**	1.00	**14**	1.00	**20**	0.40
3	0.90	**9**	1.00	**15**	0.90	**21**	0.30
4	1.00	**10**	1.00	**16**	0.80	**22**	0.30
5	1.00	**11**	1.00	**17**	0.70	**23**	0.20
6	1.00	**12**	1.00	**18**	0.60	**24**	0.10

C. Locomotion Control

Because the major focus of this paper is on investigating a realistic physics model of *C. elegans*, we chose to implement a simple central pattern generator (CPG) for locomotion control similar to the one found in [11]. The CPG works by setting the activation level for the interneuron that drives the motor neurons in the first joint, $k = 1$ at each time t using the following formula:

$$a_{k=1}(t) = \sin(\frac{2\pi}{\lambda} \times t) \tag{9}$$

where λ is the wavelength.

At each successive time step $t + \Delta t$, the wave is propagated down the body such that for $2 \leq k \leq 24$

$$a_{k+1}(t + \Delta t) = a_k(t) \tag{10}$$

The value of Δt sets the characteristic frequency of the body wave (see Table II). Initially, all of the activation levels are set to 0 and between subsequent updates the interneurons are held at their last activation level.

The actual activation levels of the motor neurons a_m are dictated by two factors: (1) the activation level of the interneuron at the joint and (2) the synaptic strength of the connection between the interneuron and the motor neurons. The following equation shows this relationship:

$$a_m = a_k \times \omega_k \tag{11}$$

In a close approximation to the cross inhibition circuit in *C. elegans*, when a_k is positive, the activation of the ventral muscles (MVL and MVR) are positive and the dorsal muscles (MDL and MDR) are 0. However, when a_k is negative, the activation of the dorsal muscles(MDL and MDR) becomes positive and the ventral muscles (MVL and MVR) are 0. The synaptic strength between the interneurons and motor neurons were determined experimentally using data derived from video analysis of the worm in motion. Table III gives the weights that were found to produce a very close approximation to the gait of the worm during forward locomotion.

IV. TUNING AND VALIDATION

The next phase of construction for the simulation was to tune and cross validate its performance against real worms. To do this, we used the *C. elegans* N2 wild type strain, which we obtained from the Caenorhabditis Genetics Center (CGC) at the University of Minnesota.

A. Materials and Methods

Maintenance and culturing of worms was performed as outlined in [3]. Worms were grown on standard NGM Lite plates with OP50 1CGJ *E. Coli* and incubated at $20°C$. The worms analyzed in these experiments were young adult worms (or, a mixture of young adult and adult worms), transferred while in L4 larval stage to freshly seeded OP50 plates the night before filming [7]. Worms were recorded on modified NGM Lite agar plates (3.0g KH2PO4, 0.5g K2HPO4, 2.0g NaCl, and Agar, without the addition of peptone or cholesterol) made specifically for the clarity of the recorded image. Worms were transferred to filming plates via a worm pick and filmed within thirty seconds of transfer, in order to take advantage of the higher locomotion activity exhibited by worms shortly after transfer. We found that this produced the most reliable and longest sustained forward locomotor activity.

Worms were filmed using a Leica S8 APO Stereomicroscope fitted with a ScopeTek MDC320 digital camera, outputting at a resolution of 1024x768 at 5 frames per second. The microscope was held at the 16x magnification setting during filming, with the illumination mirror angled to obtain images with the highest possible contrast. Individual worms were filmed for five minutes, during which the agar plate was moved manually, to re-position the worm within the microscope's field of view. A total of 487 minutes of raw video in 96 files was collected.

B. Image Processing

After collecting the video, we edited it to remove footage of anything other than forward locomotion (pirouettes, backward movement, plate repositioning, etc.) Using consumer video editing software, we manually cut the raw footage into 945 files that collectively contained around 3.75 hours or 50,000 individual frames of the worm performing forward locomotion.

To analyze this footage, we developed software, called the WormAnalyzer, that is written in Java and based on the Java Media Framework (JMF). To do this, a set of JMF processors were constructed into a processing pipeline that converted each frame of the raw color video into a set of pixel locations that describes the position of the worm's body. The WormAnalyzer software batch processes footage at about 5 times faster than real time. The analysis pipeline we constructed is similar to that described in [7] with some minor differences.

The first processor in the pipeline performs a binarization of the video using a local thresholding algorithm. This algorithm uses a sliding 3 X 3 window to determine whether a given pixel represented as 24-bit Red/Green/Blue value should be converted to black (foreground) or white (background). This processor colors the pixel black if the standard deviation of the intensity of the pixel and its surrounding pixels is greater than the mean of the entire image, or if the mean intensity of the pixel and its surrounding pixels was greater than the background pixel intensity.

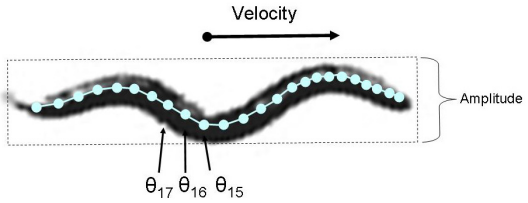

Figure 4. Features of *C. elegans* locomotion

Next, we remove small objects from the image using a region labeling algorithm that indexes each pixel in the image according to the region that it belongs to. Once all of the black regions are labeled, we remove all of the regions except for the largest. This isolates the worm (which is black) onto a white background. We then used the same method to fill holes in the worm's image by inverting the colors such that only the largest white region is maintained (the background).

With a binary image of just the background and worm in hand, we apply a triple pass thinning algorithm to reduce the worm's image down to a core body that represents the worm's basic shape [19]. This shape is often not a single line, but has multiple endpoints. We reduce it to a single line by selecting the endpoints that are furthest from one another and removing all others.

The output of this process is a set of text files, which we refer to as body files. Each body file contains one line per frame of video with each line giving a timestamp and the pixel locations of the body of the worm. The number of pixels (or length of the body) is dependent on the size of the worm and also exhibits some variability due to the binarization of the image and subsequent thinning.

Because we wanted to gather statistics based on a non-uniform segmentation of the worm's body, it was necessary to identify the location of the worm's head. To aid in this process, software was developed to show the first frame of each video file in a directory, from which a researcher could click on the head end of the worm. A head tag was then inserted into the corresponding body file that identified the location of the head in the first frame. With the head tag in place, subsequent frames of the video were properly rearranged such that the end point closest to the last head location was identified as the head. This turns out to be a very robust and reliable mechanism if the video being processed was taken at high enough frame rates.

These head-tagged body files are then post-processed in batches. The software takes a directory of head-tagged body files and produces skeleton files that provide a description of the location and position of each *segment* of the worm. Like the simulator, the size of these segments are not uniform, but are based on the muscle placement as reported in [16]. For convenience, the simulator also creates skeleton files in

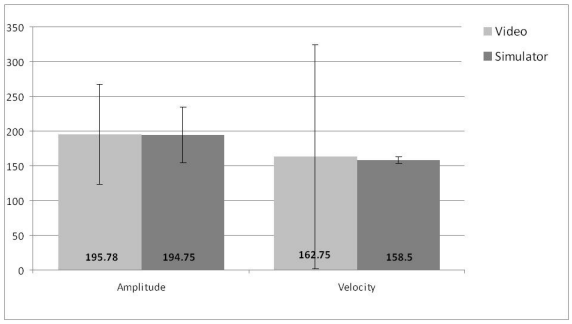

Figure 5. Comparison of locomotion velocity and amplitude of *C. elegans* to simulated results

exactly the same format as the WormAnalyzer. This allows us to directly compare the output from both processes using the same metrics calculated in exactly the same way.

The skeleton files are then processed to extract features of the worm's movement using a technique similar to the one reported in [5]. Currently, this software extracts 49 features from the worm's motion including the velocity of the centroid of the worm, the amplitude of the worm's body, the average angle at each joint location, and the angular velocity of each joint (see Figure 3). The software outputs data files that give these features on a frame by frame basis and a set of summary statistics that can be further analyzed using statistical packages.

V. Discussion

Figures 4, 5, and **??** present the results of both the analysis of the video and the simulator. The results for the video are directly in line with the results obtained in both [9] and [5]. Essentially, it can be seen that the amplitude of the body during forward locomotion is about 19.6 % of the length of the body and the instantaneous centroid velocity is about 163 $\mu m/sec$. These number are very similar to the values reported in [5], which gives a centroid velocity of 180 ± 30 $\mu m/sec$ and an amplitude of $19.27 \pm 2.34\%$.

Figures 5 and **??** show that as the wave propagates down the body that its amplitude decreases as is evident by the bend angles that are produced in these regions. This is similar to the shape of the average flex angles that are reported in [9], further validating the results of our video analysis.

When comparing the video results to the simulated results we see that, with the exception of the head and tail of the worm, our simulator accurately reproduces the velocity, amplitude, individual angles, and angular velocities of the real worm. We have analyzed the reason for the discrepancy at the head and tail and have concluded that it is caused by two factors. First, the process of analyzing the video produces variability in the length of an individual worm over even short video clips. When statistically analyzing the angles, this would have a tendency to drive the angles and velocities of these regions toward the mean values. Second, the simulation uses a worm of 100 units long with each unit representing $10\mu m$. This makes the second segment of the worm exactly 1 unit in length. When using integers to represent the location of the joints connected to this segment to calculate the angles, it allows only values that are multiples of $45°$. The same error is probably being introduced in the video analysis, but is stabilized by the variability of the worm's length. Overall, these factors effect the analysis, but not that actual behavior of the simulated worm, which by all appearances precisely reproduces the motion of the real organism.

Analytically, the frequency of the CPG used to drive our locomotion is about 0.3Hz. Even though this is within one standard deviation of the value of 0.36 ± 0.08 Hz for N2 wild type reported in [5], it is still slightly below the expected value. This is entirely expected as the velocity that we produce is slightly lower and the amplitude slightly higher than was reported in that work. We are very confident that changing the values of either λ or Δt will cause our simulation to reproduce the values they report.

We would also like to mention that the process of tuning a CPG to produce the gait of the worm was a very difficult endeavor. There were two issues that we encountered that complicated the task. First, if the weight of the synapse between the interneurons and the motor neurons are uniform, then the model has a tendency to tail whip. This is caused by a decrease in the wavelength of the wave as it propagates down the body when the worm is in motion, which causes high inertial forces to be exerted. On further investigation we found references to this decrease in wavelength in living worms [10], [1]. To compensate for this effect, we decreased the weight associated with muscles in the rear of the worm, which not only removed the tail whip, but normalized the bend angles to match those observed in the video analysis.

We believe that this indicates that during forward locomotion the worm generates most of its propulsive forces using the muscles located in the anterior. The posterior portions of the worm are likely to apply just enough force to maintain the wave and prevent a loss of energy due to drag. The physiological layout of the worm's musculature seems to support this claim as about 63% of the muscles lie anterior of the AP midline. We also believe that this has not been observed in other simulations because of the uniform representation of individual segments of the body, the lack of torsional inertial force, and the lack of explicit modeling of the friction caused by variations in surface contact.

The second issue we encountered when tuning our simulator was the timing associated with the propagation of the wave from the CPG. Because of the non-uniform placement of the muscle cells and the uniform timing of the CPG, we noticed that muscle activation is uncoordinated with the timing of the physical wave as it propagates down the worm's body. In areas where the spacing between subsequent muscles is small (near the head), the muscle

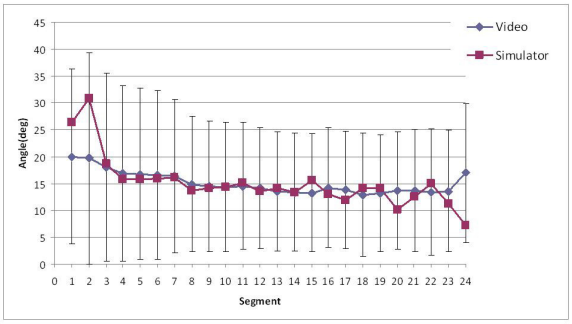

Figure 6. Comparison of bend angles in *C. elegans* to simulated results

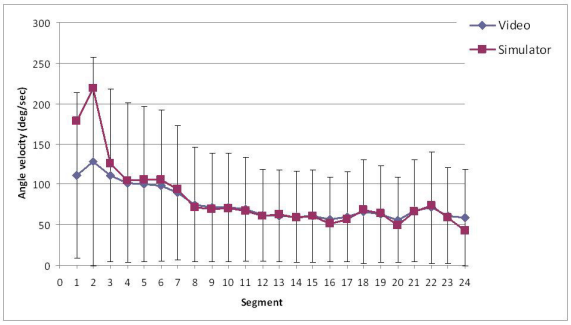

Figure 7. Comparison of bend velocities in *C. elegans* to simulated results

activation lags behind the wave and where the spacing is large, it occurs before the wave arrives (often in the tail). It is unclear how this timing issue might be resolved in the actual worm, if in fact, it uses a CPG to coordinate timing of muscle activations during locomotion. This seems to support the claim that *C. elegans* uses some form of proprioception to properly propagate the wave.

VI. Conclusion

In this paper we presented a new, biologically accurate, three dimensional model of the body of the nematode *Caenorhabditis elegans*. We tuned and validated this model against values derived from both current literature and from analysis of video recordings taken of the worm during forward locomotion. In the process of performing the tuning, we discovered two new insights into the mechanisms of locomotion employed by *C. elegans*. First, our model shows that worms may derive most of their forward propulsive force from the muscles in the anterior portion of their body with the posterior portions just propagating the wave in an energy minimizing way. Second, that the non-uniform placement of muscle cells along the body makes it difficult for a CPG to properly coordinate the timing of muscle activations with that of the physical wave as it propagates down the body.

Acknowledgment

The authors would like to thank the Caenorhabditis Genetics Center for providing the N2 strains used in this paper, Melanie Smith for insightful discussions, Mike Michalek for his assistance in editing the video files, and the members of the Rand Lab at the Oklahoma Medical Research Foundation (OMRF) for providing their protocols and support on numerous occasions.

References

[1] S. Berri, J. H. Boyle, M. Tassieri, I. A. Hope, and N. Cohen, "Forward locomotion of the nematode c. elegans is achieved through the modulation of a single gait," *HSFP Journal*, vol. 3, no. 3, pp. 186–193, 2009.

[2] J. H. Boyle, J. Bryden, and N. Cohen, "An integrated neuro-mechanical model of c. elegans forward locomotion," pp. 37–47, 2008.

[3] S. Brenner, "The genetics of caenorhabditis elegans," *Genetics*, vol. 77, pp. 71–94, 1974.

[4] J. Byden and N. Cohen, "Neural control of caenorhabditis elegans forward locomotion: the role of sensory feedback," *Biological Cybernetics*, vol. 98, pp. 339–351, 2008.

[5] C. J. Cronin, J. E. Mendel, S. Mukhtar, Y.-M. Kim, R. C. Stirbl, J. Bruck, and P. W. Sternberg, "An automated system for measuring parameters of nematode sinusoidal movement," *BMC Genetics*, vol. 6, no. 5, February 2005.

[6] M. Driscoll and J. Kaplan, *C. Elegans II*. Cold Spring Harbor Laboratory Press, 1997, ch. Mechanotransduction.

[7] W. Geng, P. Cosman, C. C. Berry, Z. Feng, and W. R. Schafer, "Automatic tracking, feature extraction and classification of c. elegans phenotypes," *IEEE Transactions on Biomedical Engineering*, vol. 51, no. 10, pp. 1811–1820, October 2004.

[8] A. V. Hill, "The heat of shortening and the dynamic constants of muscle," in *Proceedings of the Royal Society of London*, ser. B, vol. 126, 1938, pp. 136–195.

[9] J. Karbowski, G. Schindelman, C. Cronin, A. Seah, and P. Sternberg, "Systems level circuit model of c. elegans undulatory locomotion: mathematical modeling and molecular genetics," *Journal of Computational Neuroscience*, vol. 24, pp. 253–276, 2008.

[10] J. Korta, D. A. Clark, C. V. Gabel, L. Mahadevan, and A. D. T. Samuel, "Mechanosensation and mechanical load modulate the locomotory gait of swimming c. elegans," *Journal of Experimental Biology*, vol. 210, p. 23832389, 2007.

[11] E. Neibur and P. Erdös, "Theory of the locomotion of nematodes: Dynamics of undulatory progression on a surface," *Biophysics Journal*, vol. 60, pp. 1132–1146, November 1991.

[12] S.-J. Park, M. B. Goodman, and B. L. Pruitt, "Analysis of nematode mechanics by piezoresistive displacement clamp," in *Proceedings of the National Academy of Sciences*, vol. 104, no. 44, 2007, pp. 17 376–17 381.

[13] M. Powell, "Java monkey engine v2.0." [Online]. Available: http://www.jmonkeyengine.com

[14] O. S. Project, “Java monkey engine physics v2.0.” [Online]. Available: https://jmephysics.dev.java.net/

[15] R. Smith, “Open dynamics engine.” [Online]. Available: http://www.ode.org

[16] L. R. Varshney, B. L. Chen, E. Paniagua, D. H. Hall, and D. B. Chklovskii, “Structural properties of the caenorhabditis elegans neuronal network,” 2009. [Online]. Available: http://www.citebase.org/abstract?id=oai:arXiv.org:0907.2373

[17] M. Wakabayashi, “Computational plausibility of stretch recpetors as the basis for motor control in c. elegans,” 2006.

[18] W. B. Wood, *The Nematode Caenorhabditis Elegans*. Cold Springs Harbor Laboratory Press, 1988, ch. Introduction to C. Elegans Biology.

[19] T. Zhang and C. Y. Suen, “A fast parallel algorithm for thinning digital patterns,” *Communications of the ACM*, vol. 27, no. 3, pp. 236–239, March 1984.